

## Demonstration of the 101st harmonic generated from a laser-produced manganese plasma

R. A. Ganeev,<sup>1,2,\*</sup> L. B. Elouga Bom,<sup>1</sup> J.-C. Kieffer,<sup>1</sup> M. Suzuki,<sup>3</sup> H. Kuroda,<sup>3</sup> and T. Ozaki<sup>1</sup>

<sup>1</sup>*Institut National de la Recherche Scientifique, Centre Énergie, Matériaux et Télécommunications, 1650 Lionel-Boulet, Varennes, Québec, Canada J3X 1S2*

<sup>2</sup>*Scientific Association Akademprigor, Academy of Sciences of Uzbekistan, Akademgorodok, Tashkent 100125, Uzbekistan*

<sup>3</sup>*The Institute for Solid State Physics, The University of Tokyo, 5-1-5 Kashiwanoha, Kashiwa, Chiba 277-8581, Japan*

(Received 20 December 2006; revised manuscript received 19 March 2007; published 31 August 2007)

We demonstrate the generation of the 101st harmonic (wavelength  $\lambda=7.9$  nm) from manganese plasma, which is generated using the plasma high-order harmonic technique. We also investigate the variation of the high-order harmonic distribution from the manganese plasma plume as a function of the prepulse and main pulse intensities. The harmonic cutoff was at the 31st order, for pump intensities below the barrier suppression intensity for singly charged Mn ions. However, by using higher prepulse and main pulse intensities, the harmonic cutoff was extended to the 101st order, with an appearance of second plateau for harmonics higher than the 31st order. In this case, the low-order harmonics decreased in intensity, or completely disappeared, and the spectrum for wavelengths longer than 27.6 nm was dominated by plasma line emission. The origin of the harmonics appearing at this short wavelength plateau is attributed to the interaction of the intense main pump laser field with doubly charged manganese ions.

DOI: [10.1103/PhysRevA.76.023831](https://doi.org/10.1103/PhysRevA.76.023831)

PACS number(s): 42.65.Ky, 42.79.Nv

### I. INTRODUCTION

Intensive research in high-order harmonic generation (HHG) has resulted in the development of unique coherent soft x-ray sources with high brightness, extremely short pulse duration, and high spatial coherence. The majority of such studies have been performed using gas as the nonlinear medium, with the successful demonstration of harmonics with wavelength in the range of a few nanometers and pulse duration as short as hundreds of attoseconds [1]. Furthermore, recent results have shown that the interaction of relativistically intense lasers with solid surfaces can be an alternative method for HHG with wavelengths extending into the spectral water-window region [2]. However, typically observed conversion efficiencies of HHG are on the order of  $10^{-6}$ , which can be a disadvantage when considering application of harmonics.

Recent studies have shown that such low conversion efficiency can be partially overcome by using the laser-ablated plasma as the nonlinear medium. An especially interesting observation, unique for HHG from plasma plume, is the intensity enhancement of a single harmonic, attributed to resonance with a strong radiative transition. Using this phenomenon, conversion efficiencies as high as  $10^{-4}$  from the pump laser to the harmonic have been achieved [3,4]. In spite of such interesting characteristics, HHG from plasma plume generally results in a relatively low cutoff. The highest order observed so far from singly charged ions of laser plasma was the 65th harmonic ( $\lambda=12.2$  nm) produced from boron plasma [5]. To date, this photon energy observed from plasma HHG (101 eV) have fallen short compared with the well-known cutoff rule  $E_c \approx I_p + 3.17U_p$  (where  $I_p$  is the ionization potential of the atom, and  $U_p$  is the ponderomotive

potential) [6]. Rather, over-ionization processes of the plasma plume have had decisive effects for the highest observable harmonic energy. Such over-ionized plasma defocuses the main pump laser, limiting the maximum intensity, and also creates a phase mismatch between the main pump laser and the harmonics. The influence of these two processes greatly reduces the harmonic conversion efficiency, or even fully stops HHG.

Recent studies show that harmonic emission from plasma plume originates mostly from singly charged ions [7–9]. In this case, there is a linear correlation between the cutoff energy of the harmonics and the second ionization potential of the target atom [7]. As a result, there is a maximum cutoff energy that one can obtain with this method, since even the highest second ionization potentials ( $\sim 25$  eV) will limit the cutoff to about the 60th harmonics [5,10].

At the same time, harmonic emission from doubly charged ions, as opposed to singly charged ions, can in theory extend the cutoff up to much higher energies, since the barrier suppression intensity in this case is higher. However, extending the cutoff in such cases can be achieved only if one can compensate for the negative effects of self-defocusing and phase mismatch of the main pump laser, due to the presence of higher free electron density. Such a possibility of using harmonic emission from higher charged ions to generate higher-order plasma harmonics has yet to be experimentally realized for HHG from a plasma plume, while, in the case of gas-jet harmonics, it has been demonstrated, for example, with ionized Ar [11].

In this paper, we demonstrate that by optimizing the conditions of the manganese plasma plume, one can extend the cutoff of the HHG from the plasma plume to the 101st order (wavelength  $\lambda=7.9$  nm). An important technique for cutoff optimization was the analysis of time-resolved ultraviolet (uv) spectra of the plasma emission. From these data, we show that harmonics near the cutoff were generated from the interaction of the femtosecond pump laser with doubly

\*Author to whom correspondence should be addressed; r\_ganeev@issp.u-tokyo.ac.jp

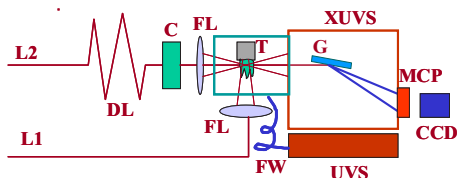


FIG. 1. (Color online) Schematic of the HHG from the manganese plasma. L1, line 1; L2, line 2; DL, delay line; C, compressor; T, target; FL, focusing lenses; xuv, xuv spectrometer; G, grating; MCP, microchannel plate; CCD, charge-coupled device; uvs, uv spectrometer; FW, fiber waveguide.

charged manganese ions, which allowed generation of 157 eV photons.

## II. EXPERIMENTAL ARRANGEMENTS

The generation of harmonics from the plasma plume requires two pump lasers, first, a long (subnanosecond) pulse to create the plasma, and a second, short (femtosecond) pulse to generate the harmonics from the plasma plume. Two temporally synchronized laser beams from a high-power Ti:sapphire laser system are necessary to independently control the characteristics of radiation (prepulse and main pulse) and to study the plasma conditions for efficient harmonic generation. For this purpose, we used the 10 Hz, multiterawatt, 35 fs beamline of the Advanced Laser Light Source [12]. The output of this beamline was configured into two beams before compression, with each beam having a maximum energy of 200 mJ and pulse duration of 210 ps. Each beam is equipped with a variable energy controller, which can independently vary the pulse energy using a computer. One of the two beams is sent to a vacuum compressor, which compresses the 210 ps pulse to 35 fs, with maximum energy of 150 mJ. We refer to the two beams used in this work as line 1 (subnanosecond prepulse; 210 ps pulse duration, 200 mJ maximum pulse energy) and line 2 (femtosecond main pulse; 35 fs pulse duration, 150 mJ maximum pulse energy).

A schematic diagram of the experimental setup is shown in Fig. 1. To create the ablation, we focused the prepulse from line 1 on to a manganese target placed in a vacuum chamber, by using a planoconvex lens (focal length  $f = 150$  mm). The focal spot diameter of the prepulse beam on the target surface was adjusted to be approximately  $600 \mu\text{m}$ . The intensity of the subnanosecond prepulse,  $I_{pp}$ , on the target surface was varied between  $7 \times 10^9 \text{ W cm}^{-2}$  to  $4 \times 10^{10} \text{ W cm}^{-2}$ . This prepulse intensity range was defined from our previous studies of HHG from different targets [13]. After some delay, part of the main (femtosecond) pulse [energy  $E = 8\text{--}25$  mJ, temporal duration  $t = 35$  fs, central wavelength  $\lambda = 800$  nm, bandwidth 40 nm (full width at half-maximum)] from line 2 was focused to the position of the plasma plume, by using a  $\text{MgF}_2$  planoconvex lens ( $f = 680$  mm). The maximum intensity of the femtosecond main pulses used in this work was  $I_{fp} = 3 \times 10^{15} \text{ W cm}^{-2}$ , above which the conditions for efficient HHG were degraded.

The harmonic spectrum was spectrally dispersed by a homemade extreme ultraviolet (xuv) spectrometer with a

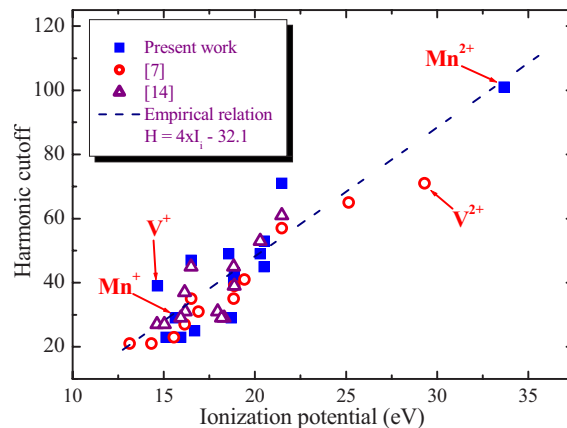


FIG. 2. (Color online) Maximum harmonic order observed as a function of the ionization potential of singly charged and doubly charged ions from various targets. The averaged line shows an empirical relation  $H$  (harmonic cutoff)  $\approx 4I_i(\text{eV}) - 32.1$ . Filled squares are the results obtained in the present work, open circles are the results obtained at the Institute for Solid State Physics, Japan [7,22], and open triangles are the results obtained at Raja Ramanna Centre for Advanced Technology, India [14].

flat-field Hitachi grating (1200 lines/mm). For detecting the xuv spectrum, we used a microchannel plate (MCP) with a phosphorus screen readout, and the image was finally recorded by a charge-coupled device (CCD). The uv spectrum emitted from the manganese plume was analyzed by a spectrometer (SpectraPro500i, Acton Research Corp.) and recorded by a time-resolved CCD camera (DH501-18F-01, Andor Technology). The 2-mm-thick, 3-mm-long Mn plates (Sigma-Aldrich, 99.9%) were used as the targets. We also compared the harmonic generation from the Mn plume and the other plasma samples (Ag, In, Au, V, Ge, Pt, Cr, Ga, Bi, Cu, Al, Pb).

## III. RESULTS AND DISCUSSION

In the present work, we observed a strong correlation between the cutoff harmonics ( $H$ ) generating from different targets and the ionization potentials ( $I_i$ ) of the particles participating in HHG, which was close to the data previously reported in Refs. [7,14]. For most targets, a linear relation was observed between the second ionization potential and the cutoff energy, implying the important role of singly charged ions for harmonic generation from the plasma plume. We confirmed this relation by comparing the reported harmonic cutoffs using main pump lasers with different pulse duration [35 fs (present study), 48 fs [14], and 150 fs [7]]. This dependence shows a linear relation between the  $H$  and  $I_i$  for targets where a harmonic plateau was observed (Fig. 2).

The above dependence is represented by the empirical relation of  $H$  (harmonic cutoff)  $\approx 4I_i(\text{eV}) - 32.1$ . From this relation, we can draw the next conclusion. When singly charged ions are strongly involved in the HHG from plasma plume, maximum harmonics are generated with targets that have higher second ionization potentials. This means that the generation of additional free electrons by further increasing

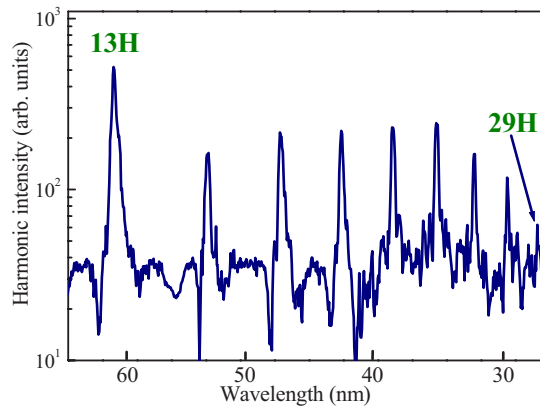


FIG. 3. (Color online) Harmonic spectrum from manganese ablation obtained at  $I_{fp}=5 \times 10^{14} \text{ W cm}^{-2}$  and  $I_{pp}=1 \times 10^{10} \text{ W cm}^{-2}$ .

the main pump intensity, due to the ionization of singly charged ions, leads to the saturation of the  $H(I_{fp})$  dependence, thus restricting the generation of higher-order harmonics.

The empirical relation was found exclusively for the specific wavelength range of the driving radiation (Ti:sapphire laser, 800 nm). This relation [ $H$  (harmonic cutoff)  $\approx 4I_i$  (eV)  $-32.1$ ] has a steeper slope than the one [ $H$  (harmonic cutoff)  $=2.5I_i$  (eV)] reported in the case of 248 nm driving pulses [15]. This seems to be consistent since a short-wavelength laser makes less significant ponderomotive energy shift. Further studies must be carried out to get insight into the mechanisms that alter the standard cutoff law ( $I_p + 3.17U_p$ ) to the empirical one by considering the role of doubly charged ions.

We could not definitely verify the participation of doubly charged ions in the HHG from the plasma plume. The three-step model predicts that, in such a case, the HHG should occur through the ionization of doubly charged ions, followed by a recombination of the electron accelerated in the laser field with the triply ionized core. In most cases, there is no need to include doubly charged ions for explaining the cutoff of the HHG from the plasma plume, since their appearance indicates a higher free electron density in the plume.

Surprisingly, the present studies of the HHG from the manganese plasma plume have revealed features related to this process. As in previous cases with other targets, we observed harmonic generation from this material up to the maximum cutoff  $H=29$ , which well coincides with the empirical rule, taking into account the second ionization potential of Mn ( $I_{2i}=15.64 \text{ eV}$ ) (see Fig. 2). The harmonic spectrum showed a conventional plateau pattern (Fig. 3). The intensity of the subnanosecond prepulse that produces the plasma plume for this case was  $I_{pp} \approx 1 \times 10^{10} \text{ W cm}^{-2}$ . However, by further increasing the subnanosecond prepulse intensity on the manganese target surface, as well as the main pulse intensity, we were able to observe a considerable increase in the harmonic cutoff. Harmonics as high as the 101st order were clearly identified in this case, though the conversion efficiency for most harmonic orders was smaller compared with the case of smaller prepulse intensities (Fig.

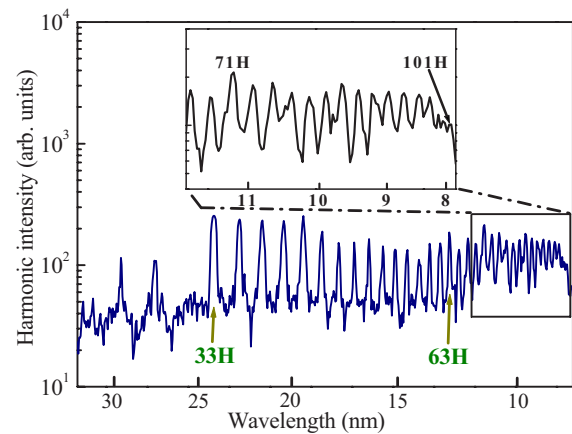


FIG. 4. (Color online) A lineout of the high-order harmonic spectrum obtained at  $I_{fp}=3 \times 10^{15} \text{ W cm}^{-2}$  and  $I_{pp}=3 \times 10^{10} \text{ W cm}^{-2}$ . Inset, a region of resolved harmonic distribution from the 67th to 101st orders.

4). An interesting observation was the emergence of a “second” plateau pattern at higher orders (from the 33rd to 93rd harmonic) with further steep drop of harmonic intensity up to 101st order ( $\lambda=7.9 \text{ nm}$ ). This second plateau appeared in place of a harmonic plateau between 15th to 29th orders that were observed for moderate irradiation of the Mn target by the subnanosecond prepulse. The observed cutoff well coincided with the empirical  $H(I_i)$  dependence, taking into account the involvement of doubly charged ions and the third ionization potential of manganese ( $I_{3i}=33.67 \text{ eV}$ ) (Fig. 2).

The similar pattern of harmonic distribution (i.e., the appearance of a second plateau) was discussed in Ref. [16]. They considered collective (plasmon) electron oscillations in laser-matter interaction and proposed the following scenario of electron movement: (a) the electron is ejected from the ground state and recombines into the same ground state, with HHG according to the three-step model [6], (b) the electron is ejected from the plasmon excited state and recombines in the ground state with HHG, thus being responsible for second cutoff, and (c) the electron is ejected from the plasmon excited state and recombines in the same plasmon excited state with HHG. Then, the electron makes an emitting transition into the ground state, thus making resonance enhancement of a single harmonic possible.

Some theoretical simulations predict that the multiplateau structure of harmonic spectra is characteristic of the weakly relativistic regime [17]. The appearance of the complex pattern in the harmonic distribution has been discussed in Ref. [18]. The second, and even the third, plateau appeared in their calculations of harmonics in the case of laser-driven tightly bound systems. They suggested that, while for neutral atoms, the low-energy part of harmonics is too short to develop any evident structure, for multiply charged ions, this part of the HHG spectrum is extensive and exhibits its own characteristic structure. However, these calculations were based on the interaction of the weakly relativistic laser intensities ( $10^{18} \text{ W cm}^{-2}$ ) with the very tightly bound hydrogen-like ions (such as  $\text{O}^{7+}$ ,  $I_p \approx 871 \text{ eV}$ ), which are quite far from our experimental conditions of the moderate laser intensities

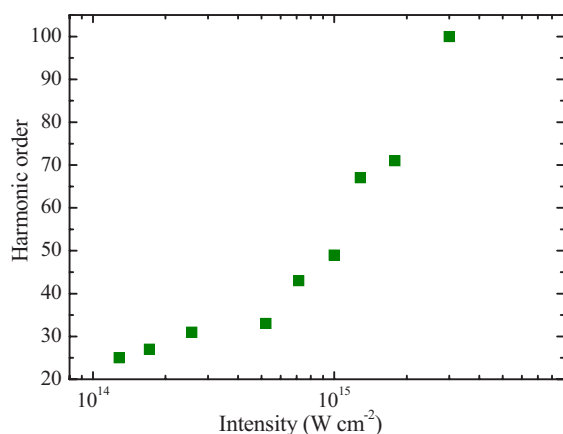


FIG. 5. (Color online) Harmonic cutoff as a function of the main pulse intensity.

and low charges of the ions ( $10^{15} \text{ W cm}^{-2}$ ,  $\text{Mn}^{2+}$ ,  $I_p \approx 34 \text{ eV}$ ). Their conditions even predicted the plateau appearance not from the “tunneling-recombination” mechanism [6,19,20], but from the inner atomic dynamics when a laser-driven bound electronic wave packet sweeps over the center of the binding potential. We are inclined to conclude that, in our case (moderate laser intensities and low-charged particles), the doubly charged manganese ions appearing during the propagation of a leading part of the pulse, as well as during further ionization of plasma by the enhanced prepulse, participate in the harmonic generation alongside with the singly charged ions, but with higher cutoff energy, which is defined by the conventional three-step model [6,19,20]. The involvement of the higher-charged species (compared to the singly charged ones) leads to the increase of the binding potential and consequently to the growth of the harmonic cutoff of the prolonged (“second”) plateau.

We performed systematic investigations of this phenomenon, by first varying the main pump intensity, and we did not observe any saturation in the harmonic cutoff with an increase in the main pulse intensity up to  $3 \times 10^{15} \text{ W cm}^{-2}$  (Fig. 5). This inferred the possibility of obtaining even higher harmonics from a manganese plasma plume, by using higher main pulse intensities. However, further growth of pump intensity led to the appearance of strong plasma emission in the xuv range caused by a considerable tunneling ionization, which overlapped harmonic emission. We should note that the highest harmonic that we could observe was restricted by the spectral resolution of our spectrometer, as well as the continuum emission from the plasma in the range of 5 to 10 nm.

Next, we performed the time-resolved spectral studies of the emission from the Mn plasma in the uv range. These results showed that, for conditions when higher-order harmonics were generated, the main laser pulse interacted with the singly charged ions, for the maximum delays used in these experiments. The doubly charged ions appeared after the leading part of the main laser started to irradiate the plume, since the main pulse intensity exceeded the barrier suppression intensity for singly charged ions. Further interaction of the main laser radiation with these ions led to their

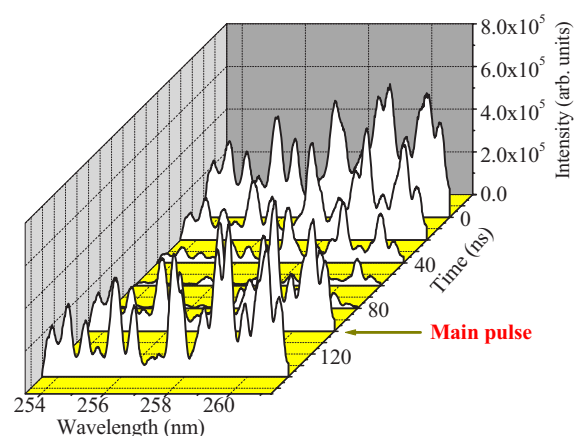


FIG. 6. (Color online) Time-resolved uv spectra of the “optimal” plasma produced on the surface of a manganese target,  $I_{pp} \approx 3 \times 10^{10} \text{ W cm}^{-2}$ .

ionization, acceleration of electrons in the laser field, and their recombination with the core, producing the emission of higher harmonics.

The time gate for each uv spectral measurement was 20 ns. Measurements were taken each 10 ns from the beginning of the irradiation of the Mn target, up to 150 ns. We performed these time-resolved measurements at both the “optimal” and “nonoptimal” conditions for HHG. We measured the change in the Mn plasma emission in the vicinity of the uv spectral lines related with the excitation of the singly charged ions (253–263 nm), where various lines could be compared within a narrow spectral range. We generated the “optimal plasma,” at which both the plateau-like distribution and the maximum cutoff were observed [at  $I_{pp} \approx (2-3) \times 10^{10} \text{ W cm}^{-2}$ ]. The term “optimal plasma” is referred to the conditions when maximum HHG conversion efficiency can be achieved by adjusting the charge state of the plasma, together with the pulse delay and focusing geometry of the femtosecond pulse. For 210 ps prepulse, the average plasma density was  $(3-4) \times 10^{17} \text{ cm}^{-3}$  at the above-mentioned prepulse intensities and 100 ns delays, which was estimated from the calculations using the HYADES code. We present in Fig. 6 the result of the change in such time-resolved spectra during the first 150 ns, for a prepulse to a main pulse delay of 100 ns.

The decay times of ionic lines at optimal conditions for harmonic generation were about 60 ns. One can see a fast decrease in the intensities of all  $\text{Mn}^+$  lines, which were excited in these conditions. In these time-resolved spectra, the main pulse arriving 100 ns after the beginning of plasma formation excites exclusively the ionic lines in the spectrum, while no increase in the intensity of the neutral lines can be observed after the interaction of the main pump laser with the plasma.

A different behavior of the uv spectrum dynamics was observed when one increases the prepulse intensity at the surface of the manganese target. An insignificant increase in the prepulse intensity from  $3 \times 10^{10}$  to  $4 \times 10^{10} \text{ W cm}^{-2}$  lead to a considerable increase in the emission from the manganese plume. Apart from an approximately fivefold growth of

TABLE I. Simulations of Mn and Au plasma characteristics at different prepulse intensities using the HYADES code.

Intensity ( $10^{10}$ W cm $^{-2}$ )	Target	1	2	3	5
Electron density ( $10^{17}$ cm $^{-3}$ )	Mn	1.3	3.25	3.77	6.13
	Au	7.32	14.2	18.5	25.2
Ion density ( $10^{17}$ cm $^{-3}$ )	Mn	1.3	3.25	3.77	4.50
	Au	4.7	6.03	6.8	7.52
Ionization level	Mn	0.62	1.0	1.0	1.36
	Au	1.56	2.35	2.72	3.35

the intensities of the ionic lines, some additional lines (associated predominantly with other ionic transitions) appeared and showed longer decay times. The time-resolved uv spectra at 90 and 100 ns showed a considerable difference in the excitation of ionic lines by the femtosecond main pump for optimal and nonoptimal conditions of the HHG. Similar behavior could be expected in the xuv range as well, though we did not measure the time-resolved spectra of plasma lines in the range of plateau-like harmonics. However, their appearance in the time-integrated xuv spectra lead to a decrease or even almost a disappearance of the “low-order” harmonics (between the 13th and 29th orders), as well as to the worsening of harmonic generation conditions at the shorter-wavelength range.

Based on the above analysis, we were able to further optimize HHG by choosing the appropriate intensities of the prepulse and main pulse. This time-resolved study of manganese plasma conditions allowed the precise identification of the range of prepulse and main pulse intensities, at which optimal harmonic generation is achieved, without the prevalent influence of free electrons on the phase mismatch and self-defocusing. In this case we were able to generate the highest harmonics from the Mn plume.

In our studies using other plasma materials, we observed the opposite influence of the prepulse intensity on HHG, when we optimized plasma conditions for achieving highest harmonic order and best conversion efficiency. In particular, in the case of the Au plume, the plateau pattern of harmonic distribution deteriorated when the prepulse energy was increased above 17 mJ, corresponding to the intensity of  $I_{pp} \approx 3 \times 10^{10}$  W cm $^{-2}$  at the target surface. The strong spectral lines from multiply ionized gold atoms appeared in the xuv spectrum when the prepulse energy was further increased, and we could not distinguish any harmonics with wavelengths shorter than 33 nm.

Laser ablation itself is a complex phenomenon, especially at relatively low laser intensities used for plasma harmonics. The behavior of laser ablation will change considerably, depending on the equation of state, ionization potential, and cohesive energy of the material. The processes that determine harmonic generation from plasma plume are complex, and may involve various factors that are not considered for gas harmonics. For example, the nonlinear medium is already weakly ionized for plasma harmonics, whose level depends on the prepulse intensity. If the free electrons density is too high, it can induce phase mismatch between the pump

laser and the harmonics, or defocusing of the pump laser. Both of these effects can reduce or stop HHG.

To understand this different behavior of the HHG process for different plasma materials, we performed simulations using the HYADES code [21]. The HYADES code is a one-dimensional, three-geometry, Lagrangian hydrodynamics and energy transport code. The electron and ion components are treated separately in a fluid approximation and are loosely coupled to each other. The diffusion approximation is used for modeling all energy transport phenomena. The degree of ionization is determined by a Saha, Thomas-Fermi, or other models.

We simulated the expansion of the manganese and gold targets interacting with the prepulse laser, and determined the electron density, ionization level, and ion density of these plumes as a function of the prepulse intensity, at a distance of 300  $\mu$ m from the target surface. Results of these calculations for 100 ns delay are summarized in Table I. One can see from the data that, already at  $1 \times 10^{10}$  W cm $^{-2}$ , there is a considerable difference in the ionization states of Mn and Au plasmas, which can lead to the difference in nonlinear optical response. At this intensity, the ionization level of Au plume becomes considerably higher than 1, which leads to the appearance of additional free electrons, due to the ionization of singly charged ions. The ratio between the electron density and ion density in gold plasma continues to increase at higher prepulse intensities, and at  $I_{pp} = 5 \times 10^{10}$  W cm $^{-2}$ , their ratio becomes higher than 4. The increase in the free electron density for the Au plume prevents efficient harmonic generation and extension of harmonic cutoff, due to the growing phase mismatch between the harmonic and pump laser waves.

The characteristics of manganese plasma under the same conditions are considerably different from those of Au. The ionization level of the Mn plume is considerably lower than that of Au under the same prepulse intensity, and doubly charged ions can only be expected at  $I_{pp} > 3 \times 10^{10}$  W cm $^{-2}$ . Therefore, the effect of free electrons on the HHG is smaller. What is especially important for HHG is that the ion density increases considerably with an increase in the prepulse intensity. As a result, the harmonics, especially near the cutoff, will increase nonlinearly in intensity, thus helping the detection of these harmonics. These combined features of relatively low electron density and high ion density in manganese plasma allowed for the demonstration of the high harmonics observed from a plasma plume.

The results show that findings in the extension of the harmonic cutoff toward the soft x-ray region may be possible, by searching for the optimal HHG conditions of the plasma plume through simulation of plasma characteristics and the time-resolved analysis of the uv spectral dynamics. Some indirect confirmation of this approach was recently found for harmonic generation from vanadium plasma. Assuming that singly charged ions ( $I_{2i}=14.65$  eV) are the highest ionization states participating in HHG, the cutoff for vanadium is estimated to be at about the 30th harmonic, according to the previously mentioned empirical relation. In fact, we were able to observe the 39th harmonic from this plume, which is in the range of uncertainty of the empirical relation presented in Fig. 2. However, recent studies have shown that the HHG from the vanadium plume at specific plasma conditions has a cutoff at considerably shorter wavelength (with harmonics demonstrated up to the 71st order [22]). Hydrodynamic simulations showed that doubly ionized atoms were present within the vanadium plasma. If we use the ionization potential of the doubly charged vanadium ions ( $I_{3i}=29.31$  eV), the maximum expected cutoff would be about the 79th harmonic. This is in a reasonable agreement with the experimentally observed cutoff (71st harmonic), especially since the estimation of the cutoff was done using the laser intensity when focusing into the vacuum. In the experiment, however, defocusing of the incoming laser beam due to plasma build-up and increase of the free electrons density is expected, thereby decreasing the effective intensity, and thus the achievable cutoff. These two results, as well as the data on harmonic generation from singly and doubly charged manganese ions, are shown in Fig. 2 assuming their corresponding ionization potentials.

#### IV. CONCLUSIONS

We have shown that doubly charged ions at appropriate plasma conditions can be used to increase the coherent photon energies obtained from ablation HHG. We were able, by optimizing plasma conditions using the time-resolved spectral analysis of the manganese plume, to generate high photon energies of harmonics from laser ablation ( $\lambda=7.9$  nm,  $E_c=157$  eV, 101st harmonic of the 800 nm radiation). In principle, harmonic generation from the doubly charged ions could be used to achieve harmonic energies of 400 eV or more by using the species with the highest third ionization potentials and higher intensity driving pulses, at appropriate plasma conditions.

The results presented in this paper reveal some expectations for further extension of the harmonic cutoff through the

generation from doubly charged ions, when the plasma conditions remain optimal for the HHG (no considerable phase mismatching due to the increase of free electron density). Such an approach, together with already demonstrated single-harmonic enhancement in the plateau region, can pave the way for further improvements in conversion efficiency and maximum cutoff energy of the high harmonics generating through the interaction of the radiation of moderate intensity ( $<3 \times 10^{15}$  W cm<sup>-2</sup>) with the laser ablation.

HHG from gas jets has already entered well into the “water window” region (2.3–4.6 nm). The question is why the result of the 101st harmonic generation (7.9 nm) from plasmas would surprise the community? The initial studies of HHG from gas jets have also shown relatively low orders of harmonics, which were further enhanced up to the present state of a few hundreds of eV photons. The presented experimental results are at the leading stage of the HHG studies using ablated plumes. Further studies can probably reveal both the higher cutoff energies and the higher harmonic yields.

The potential advantage of using plasma targets for HHG instead of normal gas jets is that one can tune to some resonances to enhance the conversion efficiency of specific harmonics at a shorter wavelength region. For these purposes, one must generate as high harmonic order as possible for further tuning to the appropriate ionic resonance at the shortest wavelength region. This is very important for HHG applications. Another question is whether resonance-tuning technique may apply to high-order harmonics? Is it restricted because of its large photon energy? To date, no resonance enhancement of high harmonics above 45 eV using the 800 nm radiation was reported [8]. However, the search of plasma species, together with new plasma configurations and experimental schemes (e.g., double-target scheme, double excitation, second harmonic excitation, etc.), could reveal new opportunities in this direction. For example, single harmonic enhancement in the range of 53 eV was recently observed in Mn plasma by using the 400 nm driving pulses [4].

#### ACKNOWLEDGMENTS

This work was partially supported by the Research Foundation for Opto-science and Technology. The authors wish to thank F. Poitras, J.-P. Moreau, and S. Payeur for their technical assistance. One of the authors (R.A.G.) gratefully acknowledges support from the Fonds Québécois de la Recherche sur la Nature et les Technologies and the invitation and support from the Institut National de la Recherche Scientifique, Énergie, Matériaux et Télécommunications to carry out this work.

- 
- [1] G. D. Tsakiris, K. Eidmann, J. Meyer-ter-Vehn, and F. Krausz, *New J. Phys.* **8**, 19 (2006).  
 [2] B. Dromey, M. Zepf, A. Gopal, K. Lankaster, M. S. Wei, K. Krushelnick, M. Tatarakis, N. Vakakis, S. Moustazis, R. Kodama, M. Tampo, C. Stoeckl, R. Clarke, H. Habara, D.

- Neely, S. Karsch, and P. Norreys, *Nat. Phys.* **2**, 456 (2006).  
 [3] R. A. Ganeev, H. Singhal, P. A. Naik, V. Arora, U. Chakravarty, J. A. Chakera, R. A. Khan, I. A. Kulagin, P. V. Redkin, M. Raghuramaiah, and P. D. Gupta, *Phys. Rev. A* **74**, 063824 (2006).

- [4] R. A. Ganeev, L. B. Elouga Bom, J.-C. Kieffer, and T. Ozaki, *Phys. Rev. A* **75**, 063806 (2007).
- [5] R. A. Ganeev, M. Baba, M. Suzuki, and H. Kuroda, *J. Appl. Phys.* **99**, 103303 (2006).
- [6] P. B. Corkum, *Phys. Rev. Lett.* **71**, 1994 (1993).
- [7] R. A. Ganeev, M. Suzuki, M. Baba, and H. Kuroda, *Appl. Phys. B: Lasers Opt.* **B81**, 1081 (2005).
- [8] R. A. Ganeev, H. Singhal, P. A. Naik, V. Arora, U. Chakravarty, J. A. Chakera, R. A. Khan, P. V. Redkin, M. Raghuramaiah, and P. D. Gupta, *J. Opt. Soc. Am. B* **23**, 2535 (2006).
- [9] R. A. Ganeev, P. A. Naik, H. Singhal, J. A. Chakera, and P. D. Gupta, *Opt. Lett.* **32**, 65 (2007).
- [10] R. Ganeev, M. Suzuki, M. Baba, H. Kuroda, and T. Ozaki, *Opt. Lett.* **30**, 768 (2005).
- [11] E. A. Gibson, A. Paul, N. Wagner, R. Tobey, S. Backus, I. P. Christov, M. M. Murnane, and H. C. Kapteyn, *Phys. Rev. Lett.* **92**, 033001 (2004).
- [12] T. Ozaki, J.-C. Kieffer, R. Toth, S. Fourmaux, and H. Bandulet, *Laser Part. Beams* **24**, 101 (2006).
- [13] L. B. Elouga Bom, J.-C. Kieffer, R. A. Ganeev, M. Suzuki, H. Kuroda, and T. Ozaki, *Phys. Rev. A* **75**, 033804 (2007).
- [14] R. A. Ganeev, H. Singhal, P. A. Naik, U. Chakravarty, V. Arora, J. A. Chakera, R. A. Khan, M. Raghuramaiah, S. R. Kumbhare, R. P. Kushwaha, and P. D. Gupta, *Appl. Phys. B: Lasers Opt.* **B87**, 243 (2007).
- [15] S. Kubodera, Y. Nagata, Y. Akiyama, K. Midorikawa, M. Obara, H. Tashiro, and K. Toyoda, *Phys. Rev. A* **48**, 4576 (1993).
- [16] J. Zanghellini, C. Jungreuthmayer, and T. Brabec, *J. Phys. B* **39**, 709 (2006).
- [17] D. B. Milošević, S. X. Hu, and W. Becker, *Phys. Rev. A* **63**, 011403(R) (2001).
- [18] S. X. Hu, A. F. Starace, W. Becker, W. Sandner, and D. B. Milošević, *J. Phys. B* **35**, 627 (2002).
- [19] J. L. Krause, K. J. Schafer, and K. C. Kulander, *Phys. Rev. A* **45**, 4998 (1992).
- [20] M. Lewenstein, P. Balcou, M. Y. Ivanov, A. L'Huillier, and P. B. Corkum, *Phys. Rev. A* **49**, 2117 (1994).
- [21] A. M. Rubenchik, M. D. Feit, M. D. Perry, and J. T. Larsen, *Appl. Surf. Sci.* **129**, 193 (1998).
- [22] M. Suzuki, M. Baba, H. Kuroda, R. A. Ganeev, L. B. Elouga Bom, and T. Ozaki, *Opt. Express* **15**, 4112 (2007).